Solution Processed AZO Thin Films Prepared from Different Source Materials

Sana Ullah[1,3*†], Fabio De Matteis[1], Massimiliano Lucci[2], Ivan Davoli[2]

[1] *Dipartimento di Ingegneria Industriale, Università degli Studi di Roma "Tor Vergata", Via del Politecnico, 1, 00133, Roma, Italy*
[2] *Dipartimento di Fisica, Università degli Studi di Roma "Tor Vergata", Via della Ricerca Scientifica, 1, 00133, Roma, Italy*
[3] *Department of Basic Sciences & Humanities, Khwaja Fareed University of Engineering & Information Technology, Abu Dhabi Road, Rahim Yar Khan, Pakistan*

Aluminum doped Zinc Oxide films were spin-coated from 1 mol% doped precursors obtained from different source materials optimizing post-deposition annealing in controlled atmospheres. AZO films were provided with pre-deposition heating at 500 °C in ambient while post-deposition rapid thermal annealing (RTA) in vacuum and in N_2-5%H_2 was provided at 400, 500 and 600 °C. Dominant ZnO c-axis oriented AZO films with typical wurtzite crystal structure were obtained. Aluminum nitrate source materials resulted in comparatively higher conductivity AZO films. We conclude post-deposition annealing in controlled environments helped increase oxygen vacancies and enhanced grain growth and crystallinity resulting in increased conductivity. Optical measurements showed an average total transmittance (%T) of about 85 % in the visible for all the films with a direct allowed band gap of about 3.2.

Keywords: AZO, Solution synthesis, Spin coating, Rapid thermal annealing, Transparent conducting oxides.

1. INTRODUCTION

Transparent metal oxides and thin conducting films are an integral part of nowadays display and touch-screen applications. Indium Tin Oxide (ITO), thanks to its low resistivity, high optical transparency and chemical stability, holds stronger the transparent conducting oxide (TCO) market. The increasing industry demands, coupled with scarce indium element resources, compel to look for alternatives. Zinc oxide (ZnO) has been looked at as an alternative and is being investigated by researched community [1]. ZnO, an otherwise insulator in its perfect crystal form, is an n-type semiconducting compound due to non-stoichiometry of intrinsic defects of oxygen vacancy and zinc interstitials. The stability of intrinsic ZnO, along with enhanced conductivity is achieved by adding elements which act as donors that replace the Zn atoms and increase free electron density, carrier concentration, or both [2]. Even the dopants, they give stability to films at high temperatures [3-4], and among different dopants, Al:ZnO, is of greater interest because of the wide availability, for the ease of doping and for the variety of preparation techniques & processes [4-7]. In this work we report on AZO thin films, prepared through solution synthesis, that avoid the complexities of the vacuum equipment. AZO films were prepared from precursors obtained using different dopant sources for aluminum. A post-deposition thermal treatment, RTA, under vacuum and under N_2-5%H_2 atmosphere for 10 minutes each at 400, 500 and 600 °C temperatures was provided. Aluminum nitrate sources along with RTA has been found to be very effective in giving higher conductivity with required optical transparency to films in comparatively short times of application keeping the thickness-es comparatively lower.

2. EXPERIMENTAL DETAILS

Zinc acetate dehydrate ($Zn(CH_3CO_2)_{2.2}H_2O$, trace metal basis, 99.999%) was used as a starting material with 2-methoxyethanol ($CH_3O(CH_2)_2OH$, anhydrous, 99.8%) (2-MEA) as solvent and mono-ethanolamine (($HOC_2H_4)NH_2$, min. 99%) (MEA) (99% min) as stabilizer. Aluminum chloride hexahydrate (AlCl3.6H2O, anhydrous, powder, 99.999%, trace metal basis) and aluminum nitrate nonahydrate (AlN3O9.9H2O, anhydrous, powder, 99.999%, trace metal basis) in 1 mol% were used as dopants. All ingredients were used as purchased from Sigma Aldrich. The starting material was dissolved in solvent, at 0.35 M concentration, and the MEA was added in molar ratio of 1:1. Solutions were stirred at 60 °C for 2 hours to obtain clear and homogeneous solutions and were brought to room temperature and aged for 2 days. Solutions were stirred again at 60 °C for 10 minutes and cooled to room temperature before deposition of films. Corning glass substrates were cleaned in an ultrasonic bath at 60°C first in acetone and then in 2-isopropanol, each for 15 minutes. After drying with N_2, substrates received a 30 minutes UV/Ozone surface activation step in a PSD-UV Novascan system. Individual layers were spin coated at 3000 rpm for 30 seconds. Successive layers received pre-deposition consolidation heating at 500 °C for 10 minutes. Post-deposition RTA was provided in vacuum and then in N_2-5%H_2 environment at 400, 500, and 600 °C for 10 minutes each to whole of film stacks.

Electrical resistance of thin films was first assessed first by measuring the sheet resistance using four-point probe method with a Jandel Engineering, UK instru-

---

* sanaullahzafar@yahoo.com
† sana.ullah@kfueit.edu.pk

ment and then calculating the resistivity by the formula $\rho = V/I \, x \, t$, where "*t*" refers to the thickness of film and "*V*" is the voltage drop across the sample at the applied current "*I*". Hall Effect measurements were carried out using HL555 LN2 CRYOSTAT system by Nanometrics to know in detail bulk resistivity, carrier concentration and mobility. The films were characterized by optical transparency in the visible using a Perkin Elmer Lambda 950 UV/VIS/NIR Spectrophotometer. Thickness of AZO films was measured using Ambios XP-200 Profilometer. The structure of films was observed by X-ray diffraction (XRD).

3. RESULTS AND DISCUSSIONS

Films intended for application as TCO are mainly characterized for electrical resistivity and optical transparency. Increased thickness could potentially result in low electrical resistivity films, but transparency would be then compromised. While very thin films are optically transparent but have higher resistivity. Here we report results for films which possess required conductivity with desired optical transparency in the visible. Comparable results vis-à-vis electrical conductivity and optical transparency were achieved keeping the thickness, amount of source materials, annealing temperatures and annealing time comparatively lower than those reported in literature for films prepared through solution synthesis [8-17].

3.1 XRD Structural Analysis

XRD analysis was carried out in the 2θ range of 0° to 80° to determine physical structure and level of crystallinity of prepared films using Panalytical X'Pert PRO diffractometer in Bragg-Brentano ($\theta/2\theta$ coupled) geometry with Cu K_α line radiation ($\lambda = 1.540598$ Å). Fig. 1 shows diffraction peaks in case of films of both dopants. All the films irrespective of the dopant and pre- and post-deposition annealing were found strongly *c*-axis oriented with characteristic ZnO hexagonal wurtzite structure and diffraction peak of crystal orientation (002) appearing at about 34.5° due to self-texturing phenomena [18].

For both the dopants, only characteristic zinc oxide diffraction peaks appeared with very much increased intensity [19] in contrast to other examples [20] where other peaks appeared as well. This shows that RTA
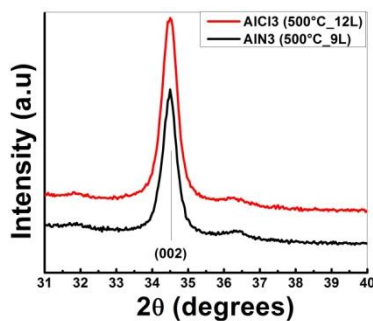

Fig. 1 – Diffraction peaks for the films of both dopants

post-deposition depress the growth of other peaks [21] and increases the growth of the characteristic peak. Also smaller width of the peak of $AlN_3O_9.9H_2O$ dopant solution in comparison to films from $AlCl_3.6H_2O$ dopant solution indicates increased grain growth with a monocrystalline character of these films. This tendered higher mobility to charge carriers and eventually reduced resistivity in case of $AlN_3O_9.9H_2O$ doped films as shown and described in sect. 3.2. We ascribe this enhanced crystallinity to the post-deposition double RTA treatment which helped enhance diffusion of dopants into the ZnO structure and increased densification of grains as is clear in SEM (sect. 3.4) analysis. This resulted in decreased porosity in the films and increased mobility of carriers. These factors were more prominent in case of $AlN_3O_9.9H_2O$ doped AZO films. All these factors helped to decrease resistivity of the films.

3.2 Electrical Measurements

The electrical resistance of the films, were first checked by a commercial multi-meter, and the ones that show, reasonable value, are better characterized by four-point method. Resistivity values were then calculated multiplying the sheet resistance by thickness of the films. To complement the measurements and confirm the resistivity values, Hall Effect electrical measurements were done to know in detail the electrical behavior of the AZO films treated with RTA temperatures in different controlled environments after preparation. Table 1 presents bulk resistivity, Hall mobility and carrier concentration in case of films with $AlCl_3.6H_2O$ & $AlN_3O_9.9H_2O$ as dopants respectively. Films were given double RTA treatment in controlled environments, first in vacuum and then in N_2-5%H_2. Thickness of the films from $AlCl3.6H2O$ precursor solutions was almost double (220 nm) in comparison to films of $AlN_3O_9.9H_2O$ (120 nm) precursors. This higher amount of material provided more than double the charge carrier concentration in the $AlCl_3.6H_2O$ precursor solution films. This higher carrier concentration however hindered the growth of grains and increased grain boundary area for $AlCl_3.6H_2O$ precursor solution films. This also increased scattering events in case of $AlCl_3.6H_2O$ precursor solution films. Hence reduced their mobility. In comparison charge carrier concentrations remained lower for $AlN_3O_9.9H_2O$ precursor solution films which reduced scattering events. This is the reason mobility of the charge carriers remained double for films from $AlN_3O_9.9H_2O$ precursor solution. This is in confirmation with the results showed by XRD analysis in sect. 3.1. RTA treatment resulted in grain growth & densification of the films. Comparatively bigger grains in case of $AlN3O9.9H2$ films resulted in reduced area of grain boundaries and hence reduced scattering. We argue that this helped increase mobility for $AlN_3O_9.9H_2$ precursor solution films. This helped to achieve higher conductivity for these $AlCl_3.6H_2O$ precursor solution films. On the other hand, carrier concentration in the range of 10^{19} cm^{-3} was achieved at half thickness for films of $AlN_3O_9.9H_2$ dopant. This helped to reduce amount of material consumption. Films of both dopant sources however showed *n*-type conductivity.

Table 1 – Resistivity, Hall mobility and carrier concentrations values for the two types of films

AlCl$_{3.6}$H$_2$O doped films (220 nm)			AlN$_3$O$_{9.9}$H$_2$O doped films (120 nm)		
Resistivity ($\Omega \cdot$cm)	Hall Mobility (cm^2/V-s)	Concentration (cm^{-3})	Resistivity ($\Omega \cdot$cm)	Hall Mobility (cm^2/V-s)	Concentration (cm^{-3})
3.710^{-3}	4.07	$-9.120 \cdot 10^{19}$	$3.02 \cdot 10^{-3}$	10.7	$-4.232 \cdot 10^{19}$

3.3 Optical Measurements

The films received similar pre- and post-deposition annealing treatments in ambient and in controlled atmospheres. The stacks were developed by successive single layer deposition. The films of both dopants however contained different number of layers so varied in thickness. Thickness of AlCl$_3$.6H$_2$O films was 220 nm while the thickness was 120 nm for AlN$_3$O$_9$.9H$_2$. Total optical transmission remained more than 80% for both films. Optical transmission obtained for both films are reported in Fig. 2. As charge carrier concentration increased, their mobility decreased as measured in electrical characterizations given in section 3.2. Higher carrier concentration with reduced mobility enhanced carrier scattering events and reduced transmission
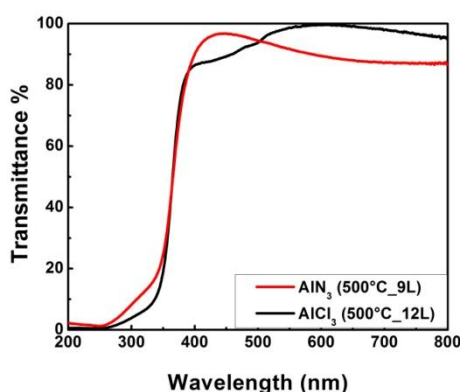
Fig.2 – Optical transmittance in case of films of both dopant solutions
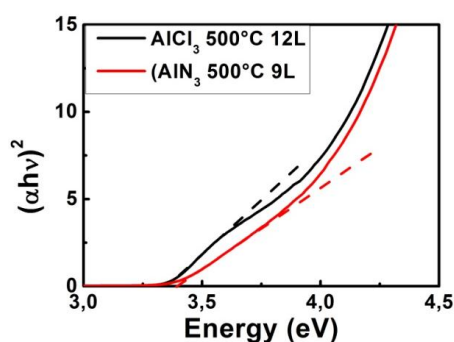
Fig. 3 – Energy band gaps as calculated from Tauc's plot for films of both the dopants

whereas higher mobility with lower carrier concentration reduced scattering events and helped increase transmission. However increased grain size due to high annealing temperatures as observed in XRD analysis when became comparable or larger than light wavelength resulted in diffusion of light and reduced trans-

mittance for films.

Oscillations in transmitted light are generated from interfaces by multiple reflections at the upper and lower interfaces of oxide films as a function of wavelength. The decrease in transmission at lower wavelengths is ascribed to optical band to band absorptions [22]. The absorption edge was calculated in Tauc plot as $(\alpha h\nu)^2$ vs. $h\nu$ for the direct allowed transition for both the films and remained a little more than 3.0 eV which is typical value for semiconducting materials.

4. CONCLUSION

In this work two group of films were prepared. The films of group 1 were prepared from precursor solution with AlN$_3$O$_{9.9}$H$_2$ as dopant and while films of group 2 were prepared from precursor solutions of AlCl$_{3.6}$H$_2$O as dopant. As pure ZnO carries oxygen vacancies and zinc interstitials as charge carriers, more of the carriers generated in case of AlCl$_{3.6}$H$_2$O dopant. However, mobility was more than double in case of AlN$_3$O$_{9.9}$H$_2$ films. Use of AlN$_3$O$_{9.9}$H$_2$ source material proved advantageous providing better conducting films at lower thicknesses reducing use of precursor materials. Rapid thermal annealing proved its efficacy in enhancing densification of films and increasing grain sizes hence reduction in resistivity. The spread out of heat in furnace tube lowers the effectiveness of the heating method. This is the reason that in case of furnace tube, longer times of annealing are normally required. RTA on the other hand, with its "direct" heating helps lower the time of application. Controlled atmospheres in the case of RTA also reduce possibility of contamination which adds to its usefulness to obtain compact thin films with high transparency & low resistivity. Better conductivity and transparent films were obtained with application of RTA for lower times of application.

REFERENCES

1. Ümit Özgür, Daniel Hofstetter, Hadis Morkoc, *Proceedings of the IEEE* **98** No 7, 1255 (2010).
2. S.J. Pearton, D.P. Norton, K. Ip, Y.W. Heo, T. Steiner, *Superlatt. Microstr.* **34**, 3 (2003).
3. Tadatsugu Minami, Hirotoshi Sato, Hidehito Nanto, Shinzo Takata, *Jpn. J. Appl. Phys.* **24** L781 (1985).
4. Hyung Jun Cho, Sung Uk Lee, Byungyou Hong, Yong Deok Shin, Jin Young Ju, Hee Dong Kim, Mungi Park, Won Seok Choi, *Thin Solid Films* **518**, 2941 (2010).
5. Yung-Chen Cheng, *Appl. Surf. Sc.* **258**, 604 (2011).
6. Deok-Kyu Kim, Hong Bae Kim, *Current Appl. Phys.* **13**, 2001 (2013).
7. S. Ullah, F. De Matteis, R. Branquinho, E. Fortunato, R. Martins, I. Davoli, *IEEE-NANO 2015 - 15th International Conference on Nanotechnology* **7388919**, 144 (2016).
8. E.J. Luna-Arredondo, A. Maldonado, R. Asomoza, D.R. Acosta, M.A. Mele´ndez-Lira, M. de la L. Olvera, *Thin Solid Films* **490**, 132 (2005).
9. Seung-Yup Lee, Byung-Ok Park, *Thin Solid Films* **484**, 184 (2005).
10. Min-Chul Jun, Jung-Hyuk Koh, *J. Electrical Eng. Technol.* **8** No 1, 163 (2013).
11. Shou-Yi Kuo, Wei-Chun Chen, Fang-I Lai, Chin-Pao Cheng, Hao-Chung Kuo, Shing-Chung Wang, Wen-Feng Hsieh, *J. Crystal Growth* **287**, 78 (2006).
12. Jin-Hong Lee, Byung-Ok Park, *Thin Solid Films* **426**, 94 (2003).
13. Jun, Min-Chul; Koh, Jung-Hyuk, *J. Nanosci. Nanotech.* **13** No 5, 3403 (2013).
14. Vrushali Shelke, M.P. Bhole, D.S. Patil, *Mater. Chem. Phys.* **141**, 81 (2013).
15. Hao Tong, Zhonghua Deng, Zhuguang Liu, Changgang Huang, Jiquan Huang, Hai Lan, Chong Wang, Yongge Cao, *Appl. Surf. Sci.* **257**, 4906 (2011).
16. S. Major, A. Banerjee, K.L. Chopra, *Thin Solid Films* **122** No 1, 31 (1984).
17. H. Deng, J.J. Russell, R.N. Lamb, B. Jiang, Y. Li, X.Y. Zhou, *Thin Solid Films* **458**, 43 (2004).
18. Shou-Yi Kuo, Wei-Chun Chen, Fang-I Lai, Chin-Pao Cheng, Hao-Chung Kuo, Shing-Chung Wang, en-Feng Hsieh, *J. Crystal Growth* **287**, 78 (2006).
19. Keh-moh Lin, Paijay Tsai, *Thin Solid Films* **515**, 8601 (2007).
20. Chi-ming Lai, Keh-moh Lin, Stella Rosmaidah, *J. Sol-Gel Sci. Technol.* **61**, 249 (2012).
21. Min-Chul Jun, Jung-Hyuk Koh, *J. Electrical Engineer. Technol.* **8** No 1, 163 (2013).
22. K.W. Liu, M. Sakurai, M. Aono, *J. Appl. Phys.* **108**, 043516 (2010).